RSC Advances

Preparation and assessment of antimicrobial properties of the bimetallic materials based on NaY zeolite

Journal:	*RSC Advances*
Manuscript ID:	RA-ART-03-2015-004960.R1
Article Type:	Paper
Date Submitted by the Author:	13-Apr-2015
Complete List of Authors:	Neves, Isabel; Universidado do Minho, Chemistry Aguiar, Cristina; University of Minho, Biology Parpot, Pier; University of Minho, Chemistry Fonseca, Antonio; University of Minho, Chemistry Ferreira, Liliana; University of Minho, Chemistry

Journal Name

RSCPublishing

ARTICLE

Preparation and assessment of antimicrobial properties of the bimetallic materials based on NaY zeolite

Cite this: DOI: 10.1039/x0xx00000x

Received 00th January 2012,
Accepted 00th January 2012

DOI: 10.1039/x0xx00000x

www.rsc.org/

Liliana Ferreira,[a] Cristina Almeida-Aguiar,[b] Pier Parpot,[a] António M. Fonseca,[a] Isabel C. Neves[a#]

The antimicrobial behavior of different pairs of bimetallic materials based on NaY zeolite was assessed in order to optimize the best metal pair composition. The materials were prepared by ion-exchange method using the zeolite Y in sodium form (NaY, 700 nm) with different metals (copper, zinc and silver). The resulting materials were characterized by Scanning Electron Microscopy (SEM), X-Ray Diffraction (XRD), Fourier Transformed Infrared spectroscopy (FTIR), cyclic voltammetry and chemical analysis, which indicated that the bimetallic metal species were effectively ion exchanged in NaY, with no modification of the zeolite structure. The antimicrobial potential of the materials was evaluated *in vitro* using the bacteria *Escherichia coli* and the yeast *Saccharomyces cerevisiae* as indicator strains. All materials showed good antimicrobial properties being the pair Zn/Ag the most active among the bimetallic materials tested. The sequence of antimicrobial activities was as follows: $Zn_{0.05}Ag$-Y > $AgZn_{0.05}$-Y > AgCu-Y = CuAg-Y > $Zn_{0.05}$Cu-Y = $CuZn_{0.05}$-Y = NaY.

Introduction

Several solid materials are reported as promising supports for antimicrobial activity. In addition to polymers,[1] silica[2] and clays,[3] zeolite structures emerge as ideal supports to accommodate one or even two metals, due to their high exchange capacity.[4-9] Zeolites are solid inorganic crystalline materials comprised of silica, aluminium and oxygen in a three-dimensional structure.[10] The aluminium ion produces a negative charge in the lattice. The net negative charge of the zeolite is balanced by the exchangeable cation to maintain the electroneutrality of the solid.[10-12] These structures with channels and cages on a nano- and subnanometer scale of strictly regular dimensions, named micropores, coupled with high surface area, chemical inertness and no toxicity, make zeolites suitable for a variety of applications ranging from catalysis,[9,13] magnetic resonance imaging,[14] drug delivery systems,[15] sensors[16] or for water treatment processes by biosorption systems.[17] Also, the zeolite pore structures are attractive for the development of metallic-based antimicrobial materials due to the slow release of metals and their regeneration by metal diminution by secondary ion-exchange.[18-22]

In all zeolite structures, the faujasite (FAU) are compatible with the introduction of more than one metal. Particularly, in the structural synthetic analogues of faujasite, the zeolite Y stabilizes the ionic state of the metal species.[18-22] In our group we have already conducted a detailed research in different zeolite structures and we have demonstrated that when silver is incorporated as cation in NaY zeolite, the faujasite structure stabilizes the oxidation state of silver ion.[23]

The common transition metals used to explore antimicrobial properties are silver (Ag), zinc (Zn) or copper (Cu).[6,24,25] Among these, Ag is the best accepted for its antimicrobial properties and has been used since antiquity.[1,18-22] Silver species are relatively inert and safe, display high thermal stability and low volatility, exhibit cytotoxicity to animal cells dependent of the silver concentration and a broad spectrum of antimicrobial properties.[4,7,25-27] As bactericidal agent, silver is commonly used as a nanoparticle (AgNP) or in its ionic form and it is generally ascribed to have more cytotoxicity towards prokaryotic cells than towards mammalian cells. However, comparative studies show that the effective toxic concentration of silver towards bacteria and human cells is almost the same.[28-30]

Studies devoted to the action of zinc or copper are not abundant, even though recent reports show their potential as antimicrobial agents against a broad spectrum of bacteria and some fungi.[6,24,25] Copper was studied in several applications as antibacterial agent for sterilizing liquids, textiles and dental materials.[31-33] Zinc ions were also reported to have antimicrobial and anti-inflammatory properties and are currently used in healthcare applications..[31,34-36] The anti-inflammatory and antimicrobial properties of these metal ions in association with the properties of silver ions may be the key to improve the antimicrobial properties of the available materials based on zeolites.

Several studies on the biocide capacity of metal ions have proposed different mechanisms of action to explain their inhibitory effect. It appears that the positive charge of metal species is fundamental for their antimicrobial activity. The electrostatic attraction between the negatively charged cell membrane and the positive charge of these

metallic species interferes with the permeability of the membrane.[6,24,37-43] Chen *et al.*[30] described the multiple mechanisms for the attachment of metal nanoparticles (MNPs) on the bacterial cell surface, which first causes cell membrane damage or permeability change following by the penetration of MNPs into the cells.

In the present study, we advance the aforementioned works in the preparation of materials based in silver with different zeolite structures[18] and in the effect of the faujasite structure in stabilization of silver species,[23] aiming to compare the antimicrobial performance of bimetallic materials with different amounts of Ag, Zn or Cu based on NaY zeolite. NaY zeolite is a three-dimensional structure with high cation exchange capacity due to sodalite and supercages cavities that are joined by oxygen bridges between the hexagonal faces.[11,12,44] Moreover, we address the two following questions (i) does the introduction of the second metal in the zeolite improves the antimicrobial activity of the material? and (ii) which bimetallic material achieves the best antimicrobial activity? For these purposes, three monometallic and six bimetallic materials based on NaY zeolite were prepared and assessed for their antimicrobial properties against both a bacteria (*Escherichia coli*) and a yeast (*Saccharomyces cerevisiae*).

Experimental

Materials and reagents

Commercial faujasite zeolite available in the sodium form (NaY zeolite, CBV100) was obtained from Zeolyst International in powder. NaY was used after a thermal treatment at 120 ºC for 12 h in an oven. Reagent grade silver nitrate ($AgNO_3$, Fisher Scientific), zinc nitrate ($Zn(NO_3)_2.4H_2O$, Merck) and copper nitrate ($Cu(NO_3)_2.3H_2O$, Riedel de Haen) were used as received. The Gram-negative bacteria *Escherichia coli* CECT423 and the yeast *Saccharomyces cerevisiae* BY4741 were obtained from the culture collection of Biology Department at the University of Minho.

Preparation of antimicrobial materials by ion exchange method

NaY zeolite was used as the parent material and was modified by ion exchange method with aqueous solutions of MNO_3, where M is silver, copper or zinc. The monometallic and bimetallic antimicrobial materials were prepared by ion exchange method as described in detail elsewhere.[18,23,45] In brief, three monometallic materials (M_1-Y) were prepared by placing the zeolite in 50 mL of solutions of the appropriate metal nitrate at 0.01 M, in an Erlenmeyer flask with a stirrer, at room temperature, during 24 h. Subsequently, the suspensions were filtered off, washed with deionized water and dried overnight at 60 ºC. Finally, the monometallic materials were calcined under air flow at 500 ºC for 8 h. Preliminary studies with the concentration solution of 0.01 M of zinc were also carried out, but the resulting materials did not show any antimicrobial activity. Thus, for the antimicrobial materials prepared and studied with this metal in the present work, the initial concentration of zinc in solution was 0.05 M. The bimetallic materials (M_1M_2-Y) were prepared by successive exchanges (0.01 M for copper and silver, and 0.05 M for zinc) with an intermediate calcination step. For the materials with silver, precautions were taken due to the light sensitivity of silver. The resulting suspension was stirred in the dark, at room temperature, during 24 h.[18]

Evaluation of antimicrobial activity of materials

The antimicrobial activity of monometallic and bimetallic materials was evaluated by an adaptation of the agar dilution method using as reference strains the Gram-negative bacteria *Escherichia coli* CECT423 and the yeast *Saccharomyces cerevisiae* BY4741. The antimicrobial materials in concentrations of 0.5; 1.0 and 2.0 mg/mL were added to Lysogeny broth (LB) supplemented with agar or to Yeast Extract Peptone Agar (YPDA) medium, depending if the microorganism to be tested was bacteria or yeast, respectively. The mixtures were subjected to ultrasonic bath for better homogenization and plated. Overnight cultures of the tested microbial strains were transferred to new culture medium, collected at mid-exponential phase, serially diluted and used in the prepared assay media. The number of colony forming units (CFU) was determined from the application of 20 µL drops of each diluted microbial culture on the surface of the respective assay medium (in triplicate), followed by incubation at 37 ºC for 24 h (bacteria) or at 30 ºC for 42 h (yeast). Control assays were performed in the absence of zeolites. Results were expressed in terms of antimicrobial efficacy of each material, a parameter calculated as 100 – (CFUMat/CFUNaY x 100) where CFUMat represents the number of CFU observed in the prepared monometallic or bimetallic materials and CFUNaY the number of CFU observed in the presence of NaY zeolite, used as control. MIC (minimum inhibitory concentration) values for all the materials were also determined against each tested microbial strain. Statistical analysis of the results was done using Microsoft Excel 2013 to compare antimicrobial test data sets by a 2 tailed homoscedastic Student's *t*-test. All the assays were performed in triplicate at least three times.

Preparation of antimicrobial bimetallic materials electrodes

In order to evaluate the oxidation state of the metals in the bimetallic materials, the modified electrodes were prepared by a previous established procedure,[46] suspending 20 mg of the material in a Nafion/water solution (180 µL Nafion/180 µL ultra-pure water). The resulting suspensions were homogenized by using an ultrasound bath and deposited on carbon Toray (CT) paper with an area of 2x2 cm^2. Finally, the carbon Toray paper was glued to the platinum wire by using conductive carbon cement (Quintech) and dried at room temperature for 24 h.

Characterization methods

Scanning electron micrographs (SEM) were collected on a LEICA Cambridge S360 Scanning Microscope. In order to avoid surface charging, samples were coated with gold in vacuum prior to analysis, by using a Fisons Instruments SC502 sputter coater. Room temperature Fourier Transform Infrared (FTIR) spectra of the samples in KBr pellets (2 mg of sample was mixed in a mortar with 200 mg of KBr) were measured using a Bomem MB104 spectrometer in the range 4000-500 cm^{-1} by averaging 20 scans at a maximum resolution of 4 cm^{-1}. Phase analysis was performed by X-ray diffraction (XRD) with a Philips PW1710 diffractometer. Scans were taken at room temperature in a 2θ range between 5 and 60°, using Cu-Kα radiation. Metal loading on zeolitic samples was evaluated according to the SMEWW 3120 method, using Inductive Coupled Plasma (ICP) on ICP-AES Horiba Jobin-Yvon model Ultima equipment and was performed at *Laboratório de Análises of the Instituto Superior Técnico, Portugal*. Voltammetric

measurements on antimicrobial materials were carried out with a potentiostat/galvanostat from Amel Instruments coupled to a microcomputer by an AD/DA converter. The Labview software (National Instruments) and a PCI-MIO-16E-4 I/O module were used for generating and applying the potential program as well as acquiring data, such as current intensities. All electrochemical studies were performed at room temperature with a three-electrode assembly including a 250 mL glass cell. A saturated calomel electrode and a platinum foil (99.95%) were used as reference and counter electrode, respectively. The cleanness of the surfaces was tested prior each experiment by recording voltammograms in the supporting electrolyte alone. All potentials were measured and reported versus the Ag/AgCl (SCE) reference electrode.

Results and Discussion

Antimicrobial materials characterization

Antimicrobial materials based on NaY zeolite with either copper, zinc or silver were obtained by ion exchange method, in order to select the best metallic pair with antimicrobial activity. This activity was assessed using the bacteria *Escherichia coli* and the yeast *Saccharomyces cerevisiae* as microbial indicator strains and expressed by the MIC values - the minimum zeolite concentration for which no microbial growth was observed.[47]

The zeolite NaY, with average particle size of 700 nm, exhibit large specific surface area 787 m^2g^{-1} and shows low total Si/Al ratio (Si/Al = 2.83) which promotes the efficiency of its ionic exchange.[13] The preparation of the materials was performed in the liquid phase by ion exchange method,[18,45] using different solutions of metal (0.01 M or 0.05 M). For example, in the case of Cu-Y it can be schematically represented as follows:

$$NaY\ (Z) + Cu^{2+}\ (aq) \rightarrow Cu\text{-}Y\ (Z) + 2\ Na^{+}\ (aq) \quad (1)$$

and, in the case of CuAg-Y as bimetallic materials:

$$Cu\text{-}Y\ (Z) + Ag^{+}\ (aq) \rightarrow CuAg\text{-}Y\ (Z) + Na^{+}\ (aq) \quad (2)$$

SEM analysis revealed that the morphology of all materials keep the typical zeolite crystals. Fig. 1 show the micrographs obtained for NaY and CuAg-Y.

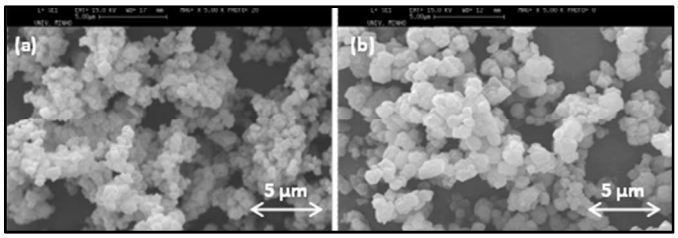

Fig. 1 SEM micrographs of (a) NaY and (b) CuAg-Y.

Analysis of the SEM micrographs of NaY (Fig. 1(a)) and CuAg-Y (Fig. 1(b)) indicates that no changes occur in the morphology and structure of the zeolite after ion-exchange treatment and subsequent calcinations. All materials retain the morphology typical of the faujasite structure with regular small particles of the parent NaY zeolite, with the average particles showing a mean diameter of 700 nm.

The results obtained by SEM are endorsed by XRD analysis. The powder XRD diffraction patterns of the parent zeolite and of all materials were recorded at 2θ values between 5 and 60º with Cu-Kα (λ= 1.5406 Å) radiation. The obtained monometallic and bimetallic materials exhibited the typical and similar pattern of the parent NaY zeolite. Fig. 2 depicts the XRD patterns obtained for NaY, Ag-Y and $AgZn_{0.05}$-Y.

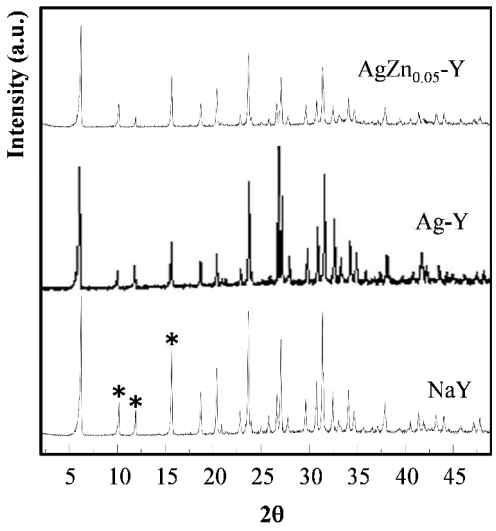

Fig. 2 XRD patterns of NaY, Ag-Y and $AgZn_{0.05}$-Y.

XRD patterns of Ag-Y and Ag $Zn_{0.05}$-Y show that the ion-exchange method does not promote structural modifications in the zeolite structure. As expected, the presence of new phases attributed to the metal species was not detected in the XRD patterns of the samples and no variation was observed in the characteristic peaks of zeolites after ion exchange, indicating that the metal species are highly dispersed in the zeolite structure.[18,23] However, a significant loss of intensity of several reflection peaks in the XRD patterns of the bimetallic materials is observed. Also, it is clear that the substitution of the sodium by the metal species change the relative intensities of some peaks (*), characteristic of faujasite structure, suggesting a redistribution of intra zeolite charge balancing cations.[18,23]

The relative cristallinity of the materials was obtained by comparing the intensities of the six peaks assigned to [3 3 1], [5 1 1], [4 4 0], [5 3 3], [6 4 2] and [5 5 5] reflections to those of the pattern of NaY, based in ASTM D 3906-80 method. For the monometallic materials, the XRD patterns of the samples present over 90 % of crystallinity. However, the reduction of the crystallinity became more significant when the zeolite was submitted to two ion-exchange treatments and subsequent calcinations. The crystallinity calculated for these catalysts ranges from over 65% for $AgZn_{0.05}$-Y to 80% for AgCu-Y.

Fourier Transformed Infrared spectroscopy (FTIR) does not reveal any significant zeolite structural modification after metal exchange, in agreement with SEM and XRD analyses. All FTIR spectra of the prepared materials are very similar, displaying the expected patterns of hydrated NaY zeolite (Fig. 3).

The presence of physisorbed water in zeolite was detected by the ν(O-H) stretching vibration at 3410 cm^{-1} with a poor resolved

shoulder at *ca.* 3600 cm^{-1} which can be attributed to the hydroxyl groups in supercages and in sodalite cages, respectively. The characteristic ν(O-H) deformation band at 1635 cm^{-1} was also observed.[18] The symmetric stretching and bending frequency bands of Al–O-Si framework of zeolite appear at 730 and 510 cm^{-1}, respectively.[18] FTIR spectra of the monometallic and bimetallic materials are dominated by the strong bands attributed to the zeolite structure. These results reveal that the zeolite structure sensitive vibrations observed are not shifted or broadening after ion exchanging which confirms that the experimental conditions used did not lead to significant modifications in zeolite structure.

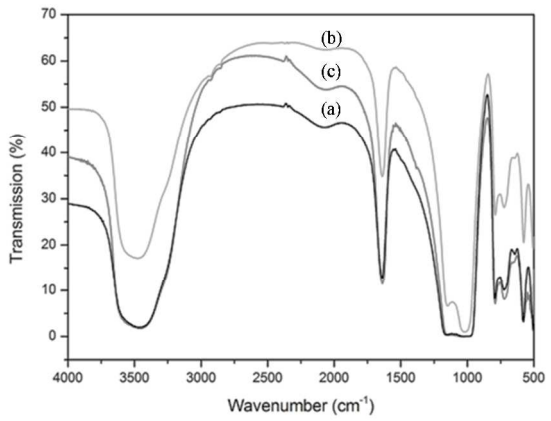

Fig. 3 FTIR spectra of NaY (a), Ag-Y (b) and $Zn_{0.05}$Ag-Y (c).

Table 1 compiles the results obtained by chemical analysis and the Si/Al ratio of the framework calculated by FTIR.[48,49] The framework Si/Al ratios determined by FTIR analysis were almost similar for all antimicrobial materials prepared and close to the ratio of the parent zeolite, indicating no expressive dealumination during the ion exchange treatments, in agreement with SEM analysis.

From chemical analysis determined by ICP, the amount of copper shifted from 0.60 in monometallic to a value around 3.0 in the bimetallic materials where copper was the second metal exchanged in zeolite. This means that in the presence of another metal in FAU structure the concentration of copper increase. Instead, the amounts of silver and zinc in bimetallic materials remain close to their amounts in monometallic materials. In these cases it seems that the second ion exchange does not improve the concentration of the second metal. The highest amount of metal was obtained for the material $Zn_{0.05}$Cu-Y, due to the higher amount of zinc.

The faujasite structure shows several positions were the cations exchanged can be located in order to compensate the negative charge of the framework .[50-52] These positions are located in the hexagonal prisms (site I), in the sodalite cages (site I' and II') or in the supercages (sites II, III and III') of the framework.[50-52] Since the ionic radius of the ions Zn^{2+} (0.74 Å) is close to Cu^{2+} (0.69 Å), probably these metal species occupied preferentially the sites I' and II.[50,51] For silver, the ionic radius is 1.14 Å, which imply that this species occupied preferentially the sites of sodalite and the supercages.[52] After the second ion exchange treatment, the metal ions will occupy the sites vacant in sodalite and supercages cavities.

Information about the oxidation state of the metals introduced by ion exchange method in NaY zeolite can be obtained by cyclic voltammetry studies. To our best knowledge, these studies are new with bimetallic materials based in zeolites and display an unequivocal proof of the presence of metal species in parent zeolite after ion-exchange treatments and subsequent calcinations.

Electrochemical behavior of NaY and mono and bimetallic catalyst based on NaY were studied by cyclic voltammetry after the deposition on carbon Toray (CT). The presence of metal in prepared catalytic material was also confirmed by this technique. The prepared modified electrodes show good stability in aqueous medium. The successive voltammograms showed good reproducibility indicating that the modified electrodes are mechanically and chemically stable.[46,53,54]

In our previous works we showed that the cyclic voltammogram of NaY/CT did not exhibit any oxidation or reduction peaks.[46,53] As expected, in the potential region of -0.5 to 1.0 V *vs.* SCE used in this work, the parent zeolite does not present any electroactive species. The enhanced electrochemical activity of monometallic materials modified electrodes has already been noticed in the literature.[46,55,56]

Table 1 Chemical analysis and FTIR results of the parent NaY and the prepared antimicrobial materials.

Antimicrobial materials	NaY	Ag-Y	AgCu-Y	$AgZn_{0.05}$-Y	Cu-Y	CuAg-Y	$CuZn_{0.05}$-Y	$Zn_{0.05}$-Y	$Zn_{0.05}$Ag-Y	$Zn_{0.05}$Cu-Y
Si/Al[a]	2.82	2.90	2.87	2.77	2.97	2.66	2.80	2.86	2.84	2.75
M (wt%)[b]	--	1.80	1.22 (Ag) 3.29 (Cu)	1.04 (Ag) 4.61 (Zn)	0.60	1.02 (Cu) 1.25 (Ag)	0.96 (Cu) 3.16 (Zn)	3.90	3.31 (Zn) 1.85 (Ag)	4.33 (Zn) 2.74 (Cu)

[a]Framework Si/Al ratio determined from FTIR using formula Si/Al=(1/χ)-1, where $\chi=3.857-0.00621\times\omega_{DR}$.[48,49]
[b]Metal loading obtained by ICP analysis.

The cyclic voltammogram of Cu-Y modified electrode shows two redox processes corresponding to the Cu(0)/Cu(I) and Cu(I)/Cu(II) couples at E_{pa} = -0.10 and 0.00 V, respectively.[46] A broad anodic peak at 0.30 V indicates more complicated redox reactions which occur on surface, involving copper oxide (Cu(II)/Cu(III)). The modified electrode also shows a reduction peak during the negative variation of potential, characteristic of the Cu(I)/Cu(0) couple at E_{pc} = -0.30 V. The results obtained for the Ag-Y modified electrode

shows the oxidation and reduction processes of silver species at respectively 0.05 V and -0.09 V, attributed to $Ag^+ Cl^- \leftrightarrow AgCl + e^-$.[55] The cyclic voltammogram of $Zn_{0.05}$-Y modified electrode indicated a quasi-reversible one-electron process (Fig. 4). Two anodic oxidation peaks, one at -0.30 V and another at -0.10 V are attributed to oxidation of Zn(0)/Zn(I) and Zn(I)/Zn(II) respectively. During the reverse scan, two reduction peaks were observed, at -0.20 V and -0.39 V corresponding to reduction of Zn(II)/Zn(I) and Zn(I)/Zn(0), respectively.[56]

In spite of the intense research in the field of monometallic materials modified electrodes based in zeolites, there are still numerous unanswered questions regarding the redox properties of this metal species in presence of a second metal in the zeolite structure.

This lack of research is partly due to difficulties on the assessment of the oxidation state of both metal species and their stabilization by the host matrix. Fig. 5 show the cyclic voltammograms of $CuZn_{0.05}$-Y and CuAg-Y modified electrodes in 0.10 M NaCl. The voltammograms of bimetallic materials show the presence of both metal species in the zeolitic structure. They are presenting similar redox processes in the same potentials observed for the monometallic materials. These results confirm that the metal species are stabilized in the zeolitic structure showing their readiness to antimicrobial activity.

Antimicrobial properties of monometallic and bimetallic materials

Assays to screen monometallic and bimetallic materials antimicrobial potential were performed at the concentrations of 0.5, 1.0 and 2.0 mg/mL. Antimicrobial efficacy, as well as the MIC value (Table 2), was calculated for each material against *E. coli* (Gram-negative bacteria) and *S. cerevisiae* (yeast).

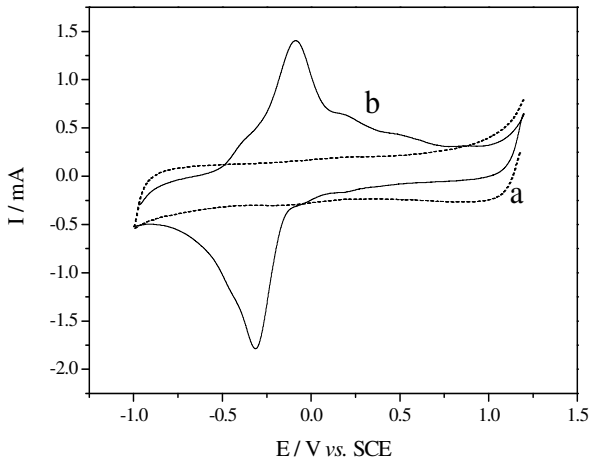

Fig. 4 Cyclic voltammograms of (a) NaY and (b) $Zn_{0.05}$-Y modified electrodes in 0.10 M NaCl.

The parent zeolite did not show microbial inhibitory effects against both microorganisms at the tested concentrations, as expected, and suggesting that the antimicrobial behavior observed (Table 2) is due to the presence of metal cations in the framework of NaY zeolite.

In our previous work, AgY was prepared using a concentration of 0.05 M $AgNO_3$ solution and MIC values of 0.2 mg/mL and 1.0 mg/mL were obtained for bacteria and yeast, respectively.[18] In this work, we used a lower concentration of $AgNO_3$ to evaluate if the introduction of a second metal in NaY is enough to compensate the decrease of Ag concentration and to preserve its antimicrobial behaviour.

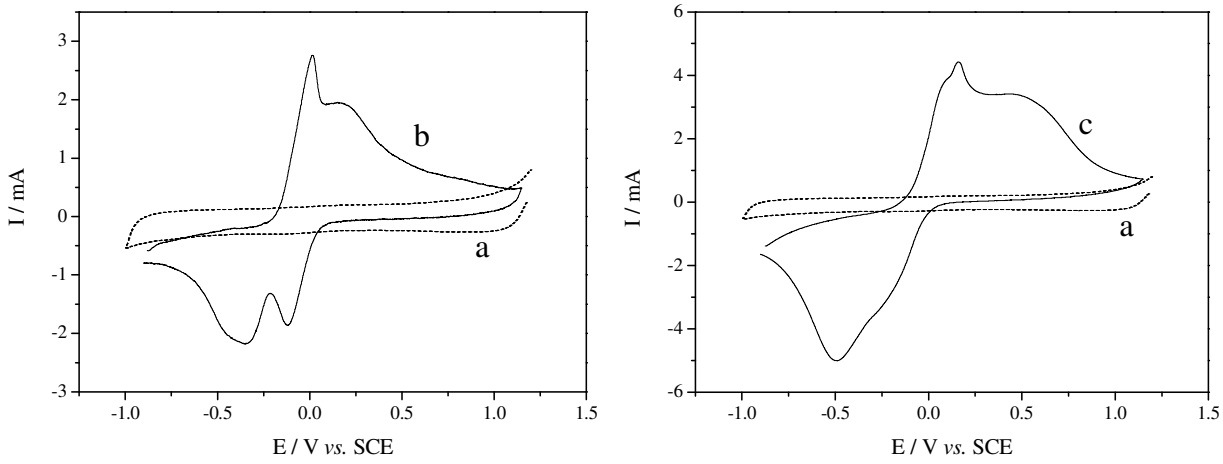

Fig. 5 Cyclic voltammograms of NaY (a) and $CuZn_{0.05}$-Y (b) modified electrodes (left) and Y (a) and CuAg-Y (c) modified electrodes (right) in 0.10 M NaCl.

Journal Name RSCPublishing

ARTICLE

Table 2 MIC values (mg/mL) for monometallic and bimetallic antimicrobial materials against the reference strains tested.

	MIC (mg/mL)									
Microorganism	**NaY**	**Ag-Y**	**AgCu-Y**	**$AgZn_{0.05}$-Y**	**Cu-Y**	**CuAg-Y**	**$CuZn_{0.05}$-Y**	**$Zn_{0.05}$-Y**	**$Zn_{0.05}$Ag-Y**	**$Zn_{0.05}$Cu-Y**
E. coli	>2	>2	1	1	>2	1	>2	>2	0.5	>2
S. cerevisiae	>2	>2	>2	2	>2	>2	>2	>2	2	>2

It can be seen that the introduction of the second metal in the zeolite plays an important role in the antimicrobial activity (Table 2). For all the monometallic materials prepared, more than 2 mg/mL of each was necessary to inhibit growth of both microorganisms whereas for most of the bimetallic materials lower MIC values were obtained (except in the case of $CuZn_{0.05}$-Y and $Zn_{0.05}$Cu-Y).

Our results suggest a synergic effect between the two metal cations in NaY structure. The incorporation of silver seems to improve the performance of all the antimicrobial bimetallic materials. In fact, the bimetallic materials with MIC values under 2 mg/mL have silver as first or second metal exchanged, which support the idea that silver is the best antimicrobial metal.[4,7,19-21,25-27] All bimetallic materials prepared showed the best results against bacteria, probably because of the simpler cellular organization of this prokaryotic organism. Fig. 6 presents the antibacterial efficacy of monometallic and bimetallic materials when tested against the Gram-negative bacteria *E. coli*. From all antimicrobial materials prepared the best MIC value was obtained for $Zn_{0.05}$Ag-Y against bacterial cells (Table 2).

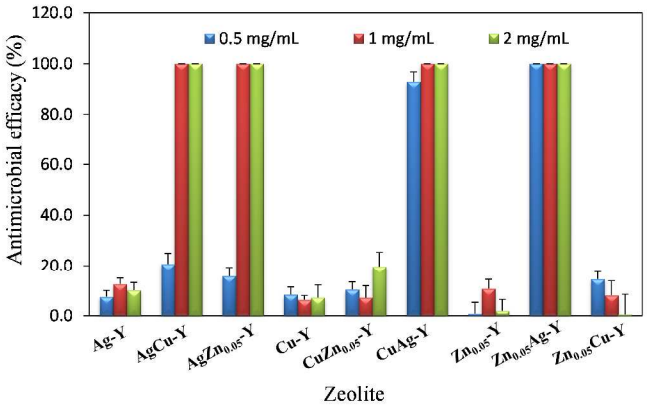

Fig. 6 Antimicrobial efficacy (%) of monometallic and bimetallic materials against the Gram-negative bacteria *E. coli*.

The results obtained with all the antimicrobial materials against the yeast *S. cerevisiae* are shown in the Fig. 7.

S. cerevisiae is more resistant to the action of zeolite doped with antimicrobial metals than *E. coli.* For almost all the materials tested, with exception of $AgZn_{0.05}$-Y and $Zn_{0.05}$Ag-Y, it was necessary more than 2 mg/mL to inhibit the growth of this microorganism. When we compare the materials $AgZn_{0.05}$-Y and $Zn_{0.05}$Ag-Y, we conclude that the MIC values against yeast are the same for both materials.

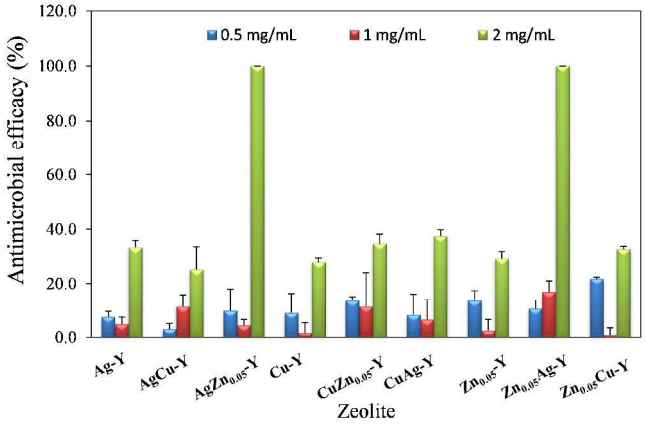

Fig. 7 Antimicrobial efficacy (%) of monometallic and bimetallic materials against the yeast *S. cerevisiae*.

However in the case of bacteria, the MIC of $Zn_{0.05}$Ag-Y is lower than the value observed for $AgZn_{0.05}$-Y. In this case, the location of silver in the positions more available in the structure enhances the slow release of the metal. The best synergetic effect of the metal species in the antimicrobial materials was obtained with the pair Zn/Ag.

These studies on the antimicrobial activity of the materials based on zeolite show that the methodology used for preparing the materials and the microorganisms tested are very important factors and highlight the need for a careful selection of such parameters to achieve a better antimicrobial performance. Nevertheless, the cytotoxicity of the prepared zeolite materials was higher towards the eukaryotic cell model than against the prokaryotic cell.

Conclusions

The obtained results reveal that the introduction of a second metal in zeolite structure plays an important role on the antimicrobial properties of a given material. Invariably, the presence of a second ion when one of the metals is silver will lead to a higher antimicrobial activity. The order of introduction of each metal in the bimetallic materials and the concentrations of the metal solutions used are factors of great importance to be considered in the optimization of the antimicrobial materials. The best results, expressed by lower MIC values, were obtained with the material $Zn_{0.05}$Ag-Y. Its antimicrobial potential, which was attributed to a synergetic effect between zinc and silver, fortify the idea that bimetallic materials can be used in substitution of many of the traditionally used organic biocides. Lower cost and toxicity are the main advantages of preparation of antimicrobial materials with a lower content in silver.

Acknowledgements

The authors are grateful to FCT (Portuguese Foundation for Science and Technology) and FEDER (European Fund for Regional Development)-COMPETE-QREN-EU for financial support to the Research Centers CQ/UM - PEst-C/QUI/UI0686/2013 (F-COMP-01-0124-FEDER-037302) and project "n-STeP - Nanostructured systems for Tail", a NORTE-07-0124-FEDER-000039 supported by Programa Operacional Regional do Norte (ON.2) - and CITAB/UM (project UID/AGR/04033/2013).

Notes and References

[a]Centre of Chemistry, Chemistry Department, University of Minho, Campus de Gualtar, 4710-057 Braga, Portugal - E-mail: (ineves@quimica.uminho.pt)
[b]CITAB (Center for the Research and Technology of Agro-Environmental and Biological Sciences), AgroBioPlant Group, Biology Department, University of Minho, Campus de Gualtar, 4710-057 Braga, Portugal

1. A. Munoz-Bonilla, M. Fernandez-Garcia, Prog Polym Sci, 2012, **37**, 281-339.
2. M. Kawashita, S. Tsuneyama, F. Miyaji, T. Kokubo, H. Kozuka, K. Yamamoto, Biomaterials, 2000, **21**, 393-398.
3. F. Ohashi, A. Oya, L. Duclaux, F. Beguin, Appl Clay Sci, 1998, **12**, 435-445.
4. P. Lalueza, M. Monzón, M. Arruebo, J. Santamaría, Mater Res Bull, 2011, **46**, 2070-2076.
5. D.R. Monteiro, L.F. Gorup, A.S. Takamiya, A.C. Ruvollo-Filho, E.R. Camargo, D.B. Barbosa, Int J Antimicrob Ag, 2009, **34**, 103-110.
6. A. Top, S. Ülkü, Appl Clay Sci, 2004, **27**, 13-19.
7. S. Sabbani, D. Gallego-Perez, A. Nagy, W.J. Waldman, D. Hansford, P.K. Dutta, Microporous Mesoporous Mater, 2010, **135**, 131-136.
8. Y. Inoue, H. Hamashima, J Biomater Nanobiotechnology, 2012, **3**, 114-117.
9. S. Chernousova, M. Epple, Angew Chem Int Ed, 2013, **52**, 1636-1653.
10. A. Corma, H. Garcia, Eur J Inorg Chem, 2004, **6**, 1143-1164.
11. Ch. Baerlocher, L.B. McCusker, D.H. Olson in: Atlas of zeolite framework types, 6th edition, Elsevier, Amsterdam, 2007.
12. L.B. McCusker, Ch. Baerlocher, Stud Surf Sci Catal, 2005, **157**, 41-64.
13. I. Kuzniarska-Biernacka, K. Biernacki, A.L. Magalhães, A.M. Fonseca, I.C. Neves, J Catal, 2011, **278**, 102-110.
14. M. Norek, I.C. Neves, J.A. Peters, Inorg Chem, 2007, **46**, 6190-6196.
15. N. Vilaça, R. Amorim, A.F. Machado, P. Parpot, M.F.R. Pereira, M. Sardo, J. Rocha, A.M. Fonseca, I.C. Neves, F. Baltazar, Colloid Surface B, 2013, **112**, 237-244.
16. I.C. Neves, C. Cunha, M.R. Pereira, M.F.R. Pereira, A.M. Fonseca, J Phys Chem C, 2010, **114**, 10719-10724.
17. B. Silva, H. Figueiredo, V.P. Santos, M.F.R. Pereira, J.L. Figueiredo, A.E. Lewandowska, M.A. Banares, I.C. Neves, T. Tavares, J Hazard Mater, 2011, **192**, 545-553.
18. L. Ferreira, A. M. Fonseca, G. Botelho, C. Almeida-Aguiar, I.C. Neves, Microporous Mesoporous Mater, 2012, **160**, 126-132.
19. C. Caroline, B.J. Carlos, B. M. L. Zapata, Z. J. Manuel, Microporous Mesoporous Mater, 2014, **188**, 118-125.
20. B. Dong, S. Belkhair, M. Zaarour, L. Fisher, J. Verran, L. Tosheva, R. Retoux, J.-P. Gilson, S. Mintova, Nanoscale, 2014, **6**, 10859-10864.
21. Y. Zhou, Y. Deng, P. He, F. Dong, Y. Xia, Y. He, RSC Adv, 2014, **4**, 5283-5288.
22. L. Tosheva, A. Brockbank, B. Mihailova, J. Sutula, J. Ludwig, H. Potgieter, J. Verran, J Mater Chem, 2012, **22**, 16897-16905.
23. A.M. Fonseca, I.C. Neves, Microporous Mesoporous Mater, 2013, **181**, 83-87.
24. R. Niira, T. Yamamoto, M. Uchida, 1990, US Patent 4938958.
25. K. Malachová, P. Praus, Z. Rybková, O. Kozák, Appl Clay Sci, 2011, **53**, 642-645.
26. Y. Inoue, M. Hoshino, H. Takahashi, T. Noguchi, T. Murata, Y. Kanzaki, H. Hamashima, M. Sasatsu, J Inorg Biochem, 2002, **92**, 37-42.
27. A. Llorens, E. Lloret, P.A. Picouet, R. Trbojevich, A. Fernandez, Trends Food Sci Tech, 2012, **24**, 19-29.
28. P.V. AshaRani, G.L.K. Mun, M.P. Hande, S. Valiyaveettil, ACS Nano, 2009, **3** (2), 279-290.
29. C. Greulich, D. Braun, A. Peetsch, J. Diendorf, B. Siebers, M. Epple, M. Kller. RSC Adv, 2012, **2**, 6981-6987;
30. C.-W. Chen, C.-Y. Hsu, S.-M. Lai, W.-J. Syu, T.-Y. Wang, P.-S. Lai, Adv Drug Deliver Rev, 2014, **78**, 88-104.
31. S. Jaiswal, P. McHale, B. Duffy, Colloid Surface B, 2012, **94**, 170-176.
32. J.P. Ruparelia, A.K. Chatterjee, S.P. Duttagupta, S. Mukherji, Acta Biomater, 2008, **4**, 707-716.
33. D. Longano, N. Ditaranto, L. Sabbatini, L. Torsi, N. Cioffi, Synthesis and Antimicrobial Activity of Copper Nanomaterials in Nano-Antimicrobials Progress and Prospects, N. Cioffi, M. Rai, (Eds.) Springer Verlag, GmbH, 2012, XVI, pp. 85-117.

34. N. Coleman, A. Bishop, S. Booth, J. Nicholson, J Eur Ceram Soc, 2009, **29**, 1109-1117.
35. A.C. Manna, Synthesis, Characterization, and Antimicrobial Activity of Zinc Oxide Nanoparticles in Nano-Antimicrobials Progress and Prospects, N. Cioffi, M. Rai, (Eds.) Springer, 2012, XVI, pp. 151-180.
36. P.C. Nagajyothi, S.J. Cha, I.J. Yang, T.V.M. Sreekanth, K.J. Kim, H.M. Shin, J Photoch Photobio B, 2015, **146**, 10-17.
37. Y. Zhang, S. Zhong, M. Zhang, Y. Lin, J Mater Sci, 2009, **44**, 457-462.
38. S. Pal, Y.K. Tak, J.M. Song, Appl Environ Microb, 2007, **73**, 1712-1720.
39. J.Y. Kim, Ch. Lee, M. Cho, J. Yoon, Water Res, 2008, **42**, 356-362.
40. Y. Zhou, M. Xia, Y. Ye, C. Hu, Appl Clay Sci, 2004, **27**, 215-218.
41. C.H. Hu, Z.R. Xu, M.S. Xia, Vet Microbiol, 2005, **109**, 83-88.
42. O. Akhavan, E. Ghaderi, Surf Coat Tech, 2010, **205**, 219-223.
43. A.M. Pereyra, M.R. Gonzalez, V.G. Rosato, E.I. Basaldella, Prog Org Coat, 2014, **77**, 213-218.
44. Database of Zeolite Structures from the International Zeolite Association (IZA-SC). www.iza-structure.org/databases/.
45. A. Jodaei, D. Salari, A. Niaei, M. Khatamian, N. Çaylak, Environ Technol, 2011, **32**, 395-406.
46. P. Parpot, C. Teixeira, A.M. Almeida, C. Ribeiro, I.C. Neves, AM. Fonseca, Microporous Mesoporous Mater, 2009, **117**, 297-303.
47. J. Hindler, Clinical Microbiology Procedures Handbook, American Society for Microbiology, Washington DC, USA, 2004.
48. W. Lutz, C.H. Ruscher, D. Heidemann, Microporous Mesoporous Mater, 2002, **55**, 193-202.
49. G.F. Ghesti, J.L. de Macedo, V.C.I. Parente, J.A. Dias, S.C. L. Dias, Microporous Mesoporous Mater, 2007, **100**, 27-34.
50. S.M. Seo, W.T. Lim, K. Seff, J Phys Chem C, 2012, **116**, 963-974.
51. K. Seff, J Phys Chem B, 2005, **109**, 13840-13841.
52. Y.M. Lee, S.J. Choi, Y. Kim, K. Seff, J Phys Chem B, 2005, **109**, 20137-20144.
53. A.M. Fonseca, S. Gonçalves, P. Parpot, I.C. Neves, Phys Chem Chem Phys, 2009, **11**, 6308-6314.
54. I. K.-Biernacka, O. Rodrigues, M.A. Carvalho, P. Parpot, K. Biernacki, A.L. Magalhães, A. M. Fonseca, I.C. Neves, Eur J Inorg Chem, 2013, **15**, 2768-2776.
55. Z.J. Jiang, C.Y. Liu, Y. J. Li, Chem Lett, 2004, **33**, 498-499.
56. A.M. Bond, A. Bobrowski, F. Scholz, J Chem Soc Dalton Trans, 1991, 411-416.

